Online Supplement

Tumor cell-derived Angiopoietin-2 promotes metastasis in melanoma

Ashik Ahmed Abdul Pari, Mahak Singhal, Corinne Hübers, Carolin Mogler, Benjamin Schieb, Anja Gampp, Nicolas Gengenbacher, Louise E Reynolds, Dorothee Terhardt, Cyrill Géraud, Jochen Utikal, Markus Thomas, Sergij Goerdt, Kairbaan Hodivala-Dilke, Hellmut G. Augustin , Moritz Felcht

A

Type of analysis/specimen	ANGPT2 detected	ANGPT2 non-detected
IHC	26	42
Primary tumor	9	9
Metastasis	17	33
ISH	47	86
Nevus	0	8
Primary tumor	4	29
Metastasis	43	49

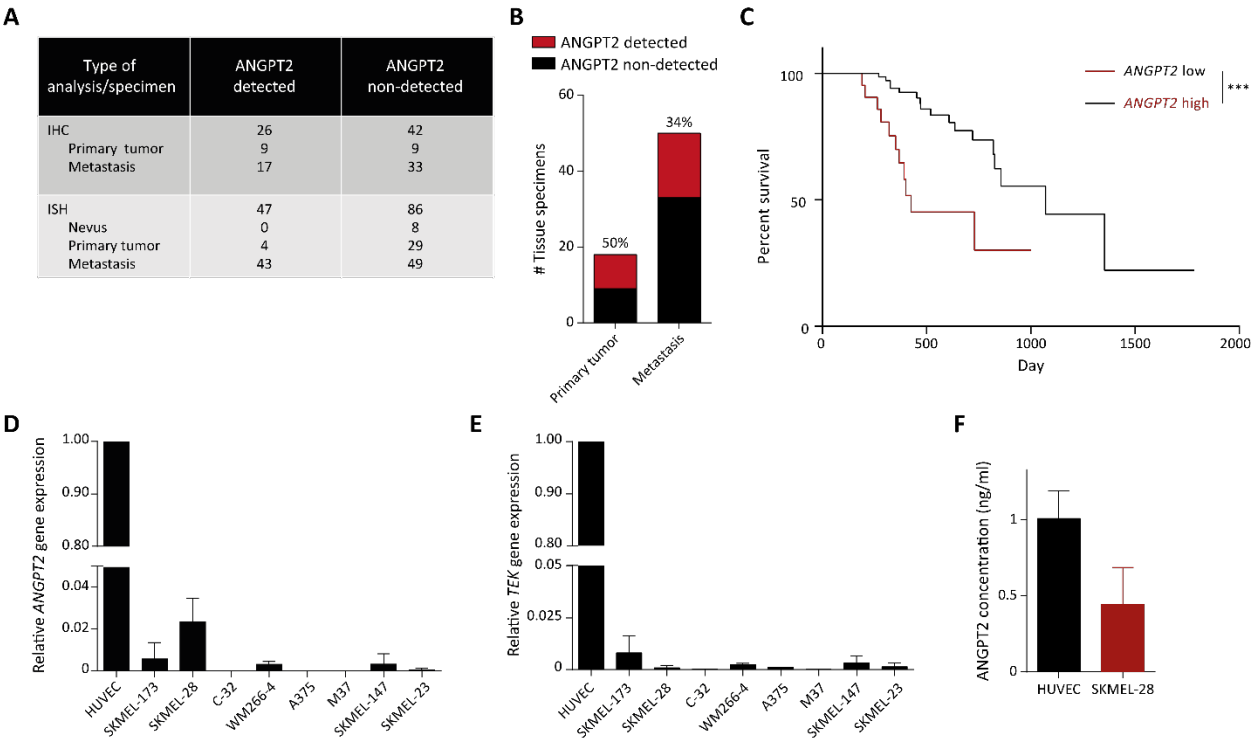

Supplementary figure S1. Melanoma cells express ANGPT2. (A) Table depicting the number of clinical specimens tested positive/negative for ANGPT2 expression from the analyzed tissue microarrays. **(B)** Quantitation of patients expressing ANGPT2 in primary (n=18) and metastatic tumor sections (n=50) determined by IHC. **(C)** Kaplan-Meier graph comparing percent survival between patients expressing either high (n=79) or low *ANGPT2* (n=23). ***, P<0.001. Log-rank (Mantel-Cox) test. **(D)** *ANGPT2* expression in different human melanoma cells quantified using qRT-PCR. The data are normalized to *ANGPT2* expression in HUVEC (n=3-4; mean ± SD). **(E)** *TEK* expression in different human melanoma cells quantified using qRT-PCR. The data are normalized to *TEK* expression in HUVEC (n=2-3; mean ± SD). **(F)** ELISA to quantify ANGPT2 in culture supernatants of HUVEC and SKMEL-28 cells (n=3; mean ± SD).

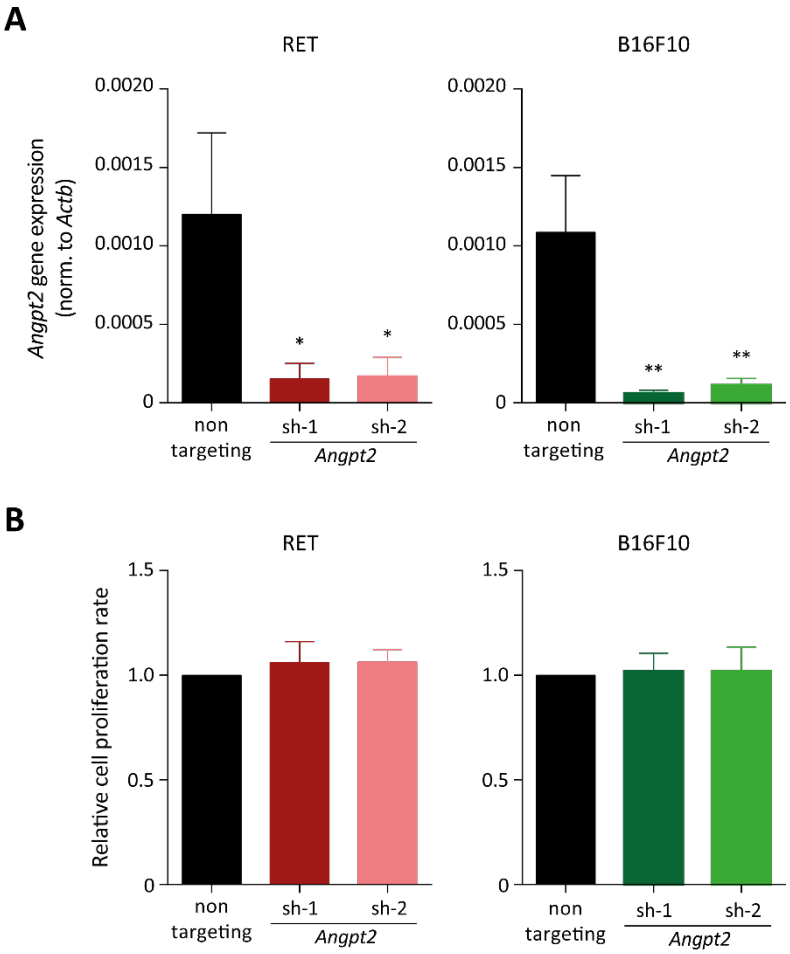

Supplementary figure S2. Melanoma cell-expressed *Angpt2* does not modulate tumor cell proliferation. **(A)** Lentivirus-mediated knockdown of *Angpt2* in RET and B16F10 cells using two independent shRNAs (sh-1 and sh-2) (n=3; mean ± SD). *, p<0.05, **, p<0.01, two-tailed unpaired Student's t-test. **(B)** MTT-based cellular proliferation assay performed with control and *Angpt2* knockdown cells (n=3; mean ± SD).

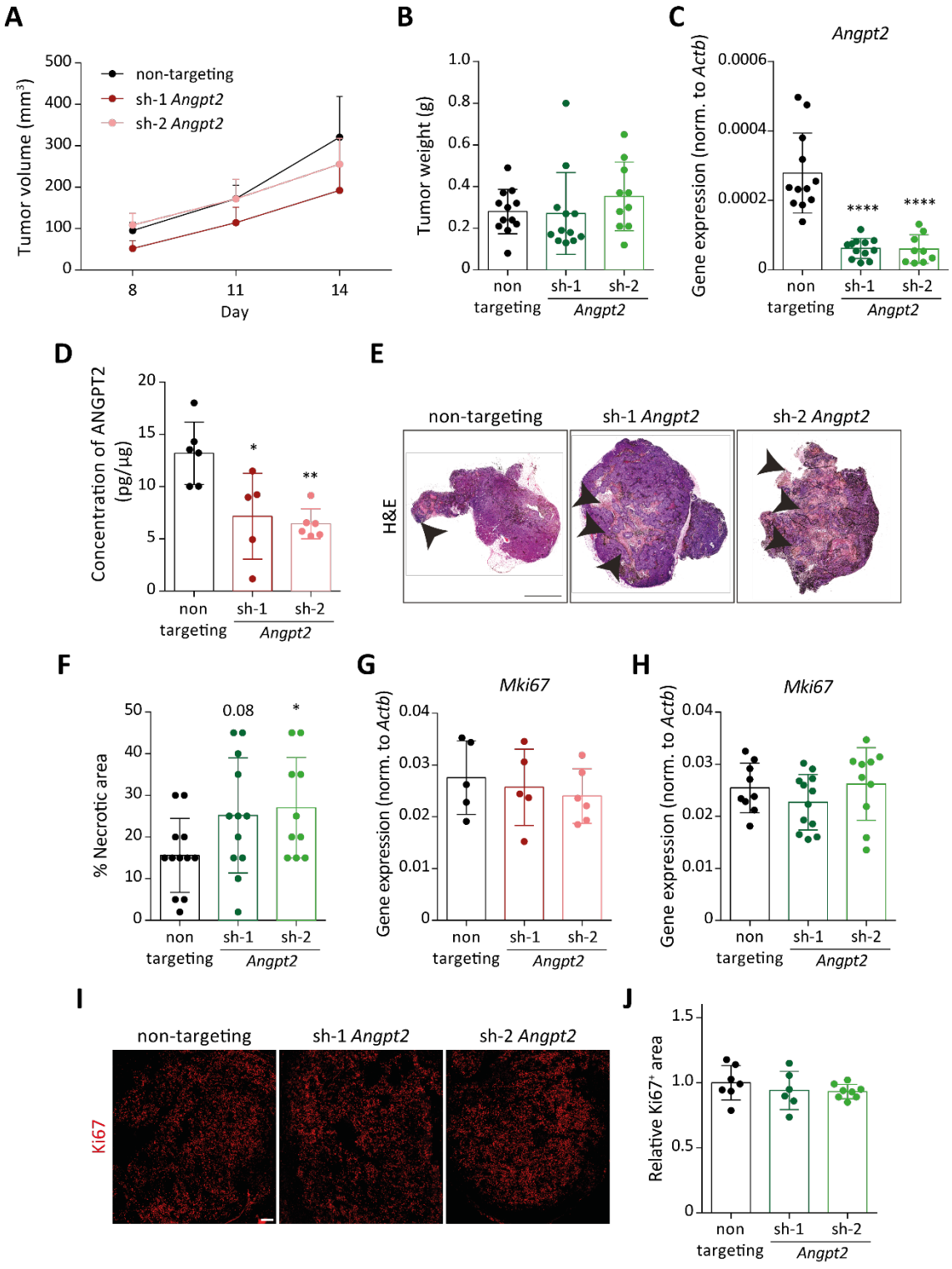
A
Tumor volume (mm³)
non-targeting
sh-1 Angpt2
sh-2 Angpt2
Day
B
Tumor weight (g)
non targeting
sh-1
sh-2
Angpt2
C
Angpt2
Gene expression (norm. to Actb)
****
****
D
Concentration of ANGPT2 (pg/μg)
*
**
E
non-targeting
sh-1 Angpt2
sh-2 Angpt2
H&E
F
% Necrotic area
0.08
*
G
Mki67
Gene expression (norm. to Actb)
H
Mki67
Gene expression (norm. to Actb)
I
non-targeting
sh-1 Angpt2
sh-2 Angpt2
Ki67
J
Relative Ki67⁺ area

Supplementary figure S3. Tumor cell knockdown of *Angpt2* does not impact growth of primary tumors. **(A)** Growth kinetics of control (non-targeting) and *Angpt2*-knockdown (sh-1 and sh-2) RET tumors (n=6; mean ± SEM). The comparison was rendered non-significant by 2-way ANOVA with Bonferroni's multiple comparison test. **(B)** Tumor weight at day 14 after inoculation of control and *Angpt2*-deficient B16F10 cells (n=10-12; mean ± SD). **(C)** *Angpt2* expression in control and *Angpt2* knockdown B16F10 primary tumors quantified by qRT-PCR (n=9-12; mean ± SD). ****, p<0.0001, Mann Whitney U test. **(D)** ELISA-based measurements of ANGPT2 concentration in either non-targeting control or knockdown RET primary tumors (n=5-6; mean ± SD). *, p<0.05; **, p<0.01, Mann Whitney U test. **(E)** Representative H&E images of control and *Angpt2* knockdown B16F10 primary tumors are shown. Arrowheads indicate necrotic area. Scale bar: 2mm. **(F)** Quantitation of intratumoral necrotic area (n=10-12; mean ± SD). *, p<0.05, Mann Whitney U test. **(G)** *Mki67* expression in control and *Angpt2* knockdown RET primary tumors as quantified using qRT-PCR (n=5-6; mean ± SD). **(H)** *Mki67* expression in control and *Angpt2* knockdown B16F10 primary tumors as quantified using qRT-PCR (n=9-12; mean ± SD). **(I)** Representative images of tissue sections from control and *Angpt2* knockdown B16F10 primary tumors stained with KI67 (in red). Scale bar: 200μm. **(J)** Quantitation of KI67-positive area normalized to DAPI area in control and *Angpt2* knockdown B16F10 primary tumors (n=6-8; mean ± SD).

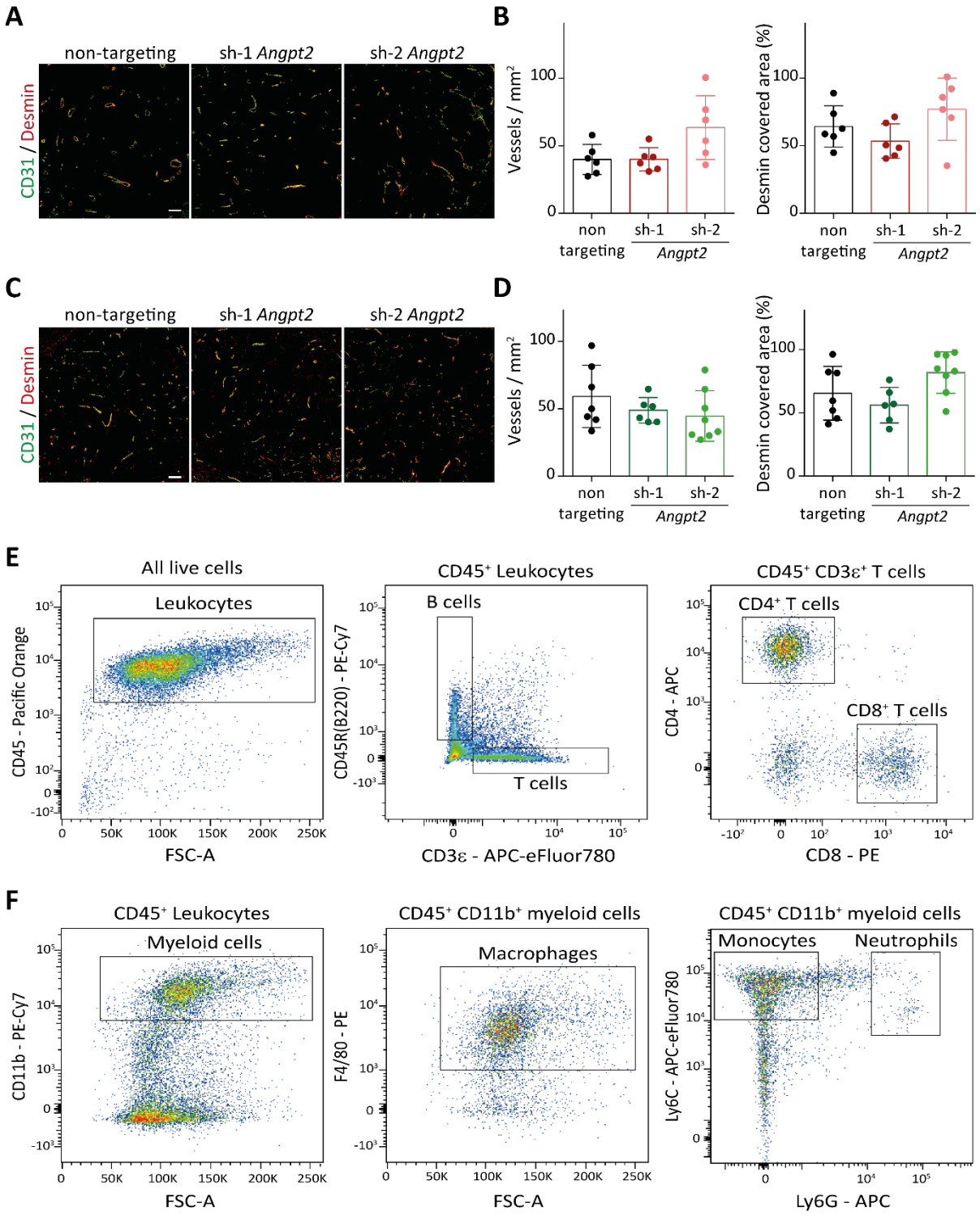
A
non-targeting
sh-1 Angpt2
sh-2 Angpt2
CD31 / Desmin
B
Vessels / mm²
Desmin covered area (%)
non targeting
sh-1
sh-2
Angpt2
C
D
E
All live cells
Leukocytes
CD45 - Pacific Orange
FSC-A
CD45⁺ Leukocytes
B cells
T cells
CD45R(B220) - PE-Cy7
CD3ε - APC-eFluor780
CD45⁺ CD3ε⁺ T cells
CD4⁺ T cells
CD8⁺ T cells
CD4 - APC
CD8 - PE
F
CD45⁺ Leukocytes
Myeloid cells
CD11b - PE-Cy7
CD45⁺ CD11b⁺ myeloid cells
Macrophages
F4/80 - PE
Monocytes
Neutrophils
Ly6C - APC-eFluor780
Ly6G - APC

Supplementary figure S4. *Angpt2*-depletion in melanoma cells does not affect primary tumor microenvironment. (A) Representative images of RET tumor sections co-stained with CD31 (in green) and Desmin (in red). Scale bar: 200µm**. (B)** Quantitation of vessel density and Desmin coverage in control and *Angpt2* knockdown RET primary tumors (n=6; mean ± SD). **(C)** Representative images of B16F10 tumor sections co-stained with CD31 (in green) and Desmin (in red). Scale bar: 200µm**. (D)** Quantitation of vessel density and Desmin coverage in control and *Angpt2* knockdown B16F10 primary tumors (n=6-8; mean ± SD). **(E-F)** Representative FACS plots depicting FACS gating strategy for analysis of tumor-infiltrating lymphoid **(E)** and myeloid **(F)** cells.

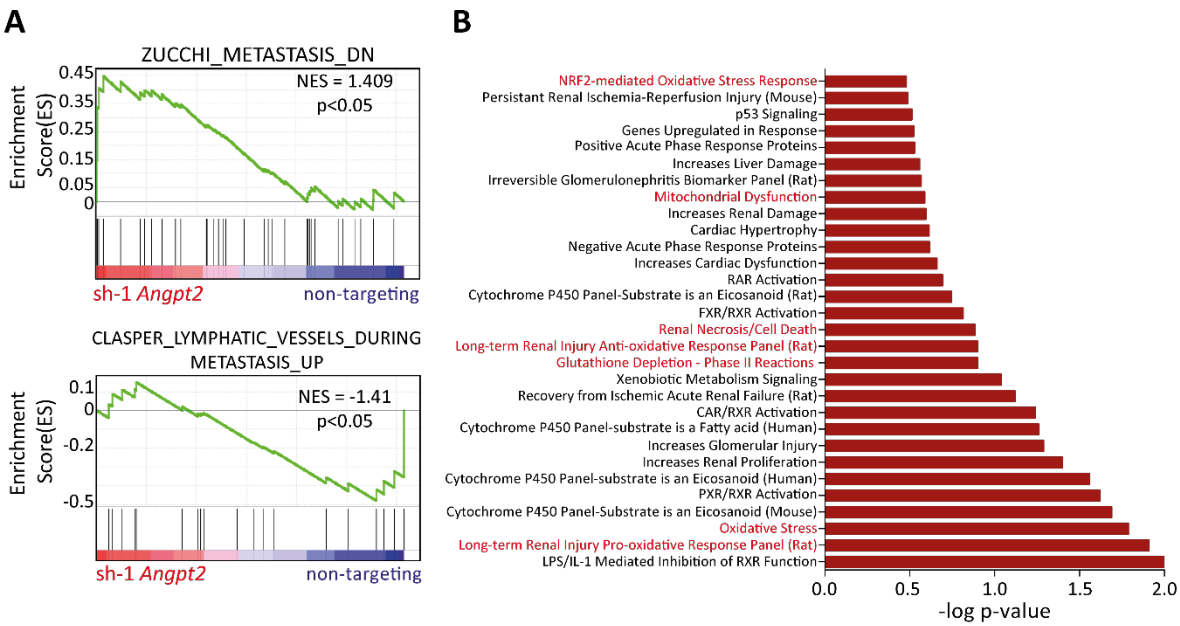

Supplementary figure S5. *Angpt2*-depletion alters pathways governing metastasis and oxidative stress. (A) GSEA plots showing regulated metastasis-related pathways in *Angpt2*-depleted tumor cells. **(B)** IPA analysis for toxicological functions with the identified differentially-expressed genes in *Angpt2*-depleted cells.

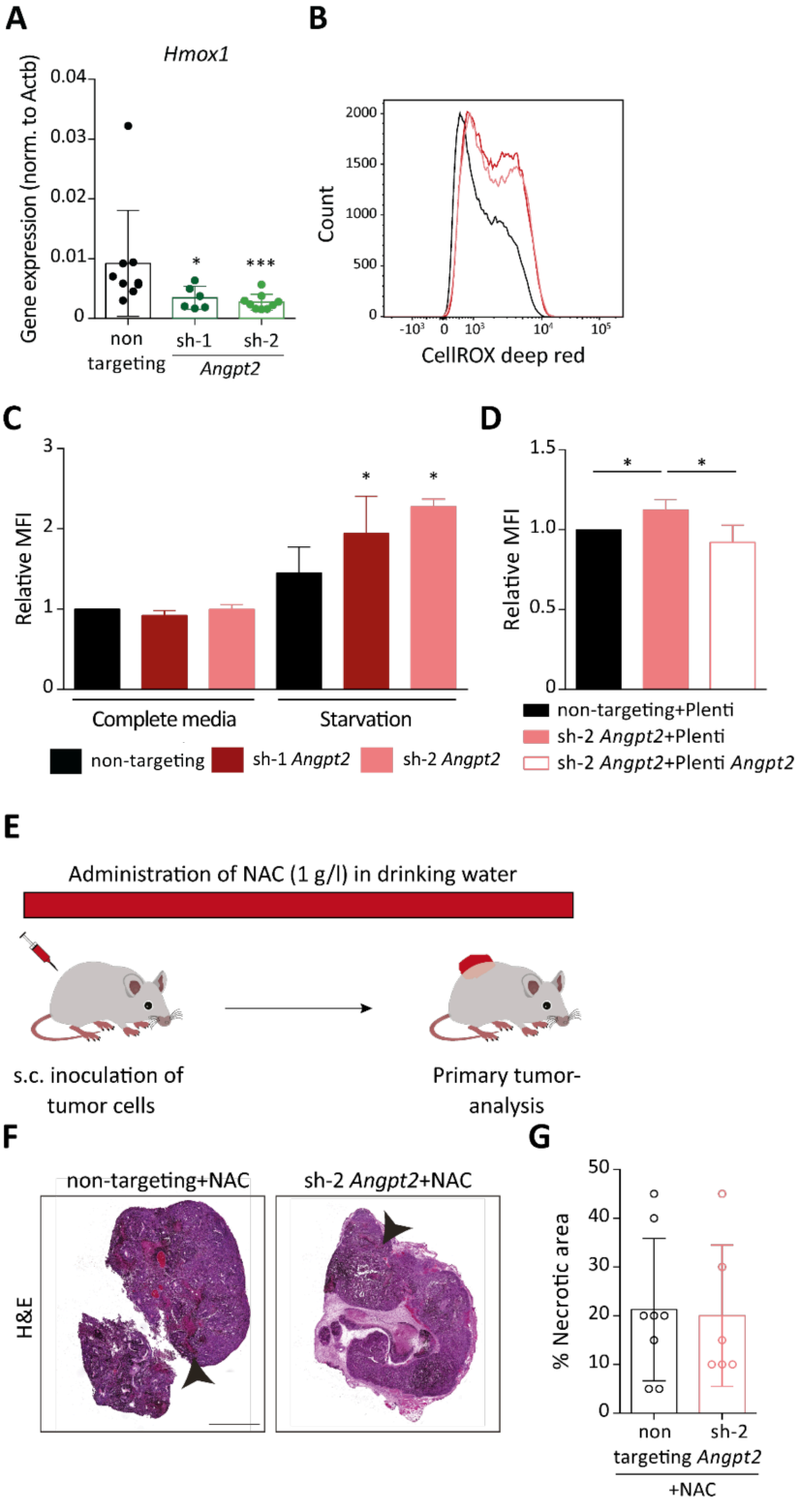
A
Hmox1
Gene expression (norm. to Actb)
0.04
0.03
0.02
0.01
0
*
***
non targeting
sh-1
sh-2
Angpt2
B
Count
2000
1500
1000
500
0
CellROX deep red
C
Relative MFI
3
2
1
0
*
*
Complete media
Starvation
non-targeting
sh-1 Angpt2
sh-2 Angpt2
D
Relative MFI
1.5
1.0
0.5
0
*
*
non-targeting+Plenti
sh-2 Angpt2+Plenti
sh-2 Angpt2+Plenti Angpt2
E
Administration of NAC (1 g/l) in drinking water
s.c. inoculation of tumor cells
Primary tumor-analysis
F
non-targeting+NAC
sh-2 Angpt2+NAC
H&E
G
% Necrotic area
50
40
30
20
10
0
non targeting
sh-2 Angpt2
+NAC

Supplementary figure S6. *Angpt2* knockdown in tumor cells affects the cellular redox balance. (A) *Hmox1* expression in control and *Angpt2* knockdown B16F10 primary tumors was quantified using qRT-PCR (n=6-9; mean ± SD). *, p<0.05, ***, p<0.001, Mann Whitney U test. **(B)** Representative histograms showing CellROX expression profile of control and *Angpt2*-depleted RET primary tumors. **(C)** Quantitation of ROS levels in control and *Angpt2*-depleted RET tumor cells under complete medium (10% FCS) and starvation (serum starved) conditions (n=4; mean ± SD). *p<0.05, two-tailed paired Student's t-test. **(D)** Quantitation of ROS levels in control+Plenti, sh-2+Plenti and sh-2+Plenti *Angpt2* RET tumor cells under starvation conditions (n=5; mean ± SD). *p<0.05, two-tailed paired Student's t-test. **(E)** Schematic representation of the rescue experiment to investigate the influence of ROS on intratumoral necrosis in *Angpt2*-depleted tumors. **(F)** Representative H&E images of control and *Angpt2* knockdown RET primary tumors treated with NAC are shown. Arrowheads indicate necrotic area. Scale bar: 2mm. **(G)** Quantitation of intratumoral necrotic area (n=6-8; mean ± SD).

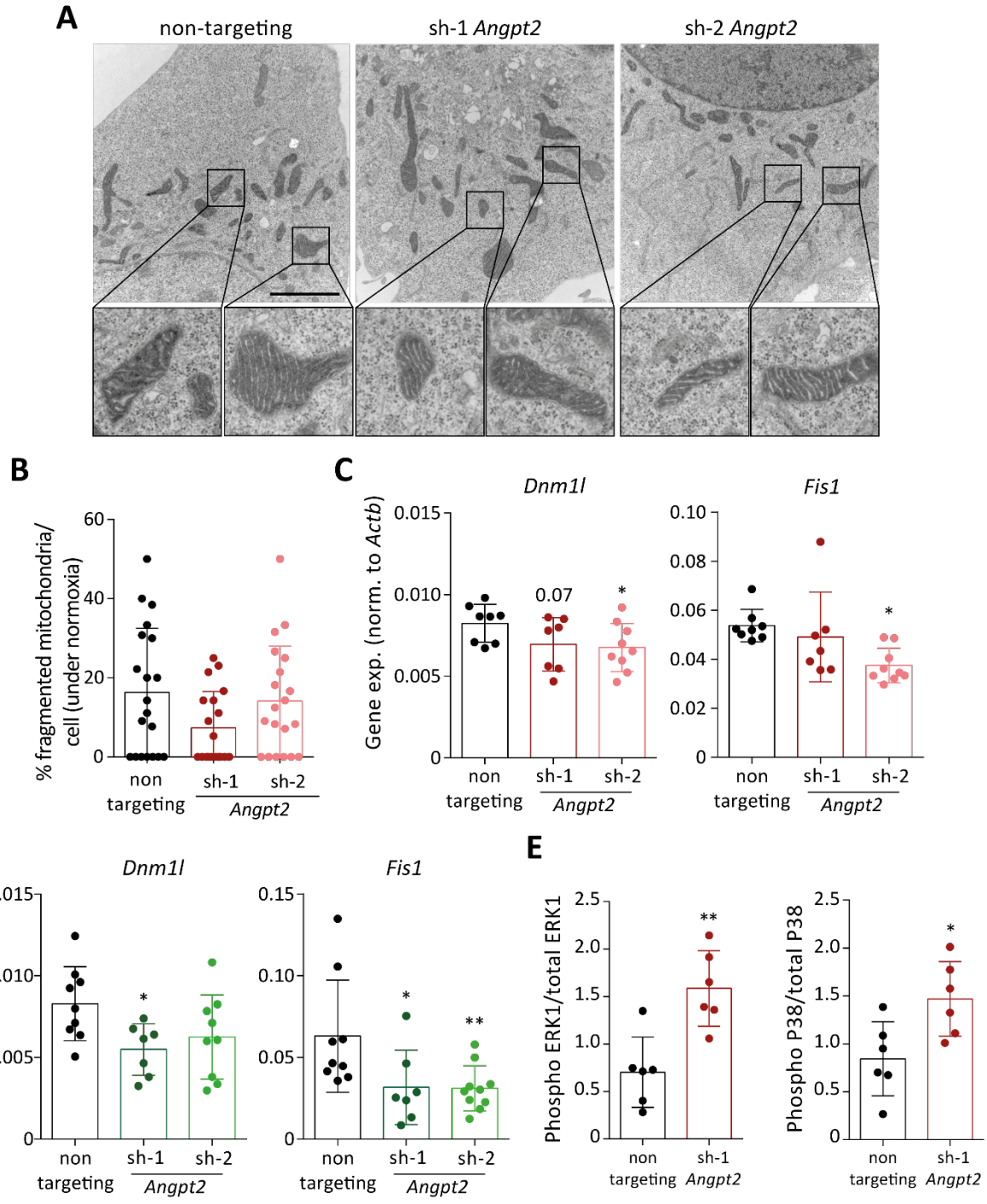
A
non-targeting
sh-1 Angpt2
sh-2 Angpt2
B
% fragmented mitochondria/ cell (under normoxia)
60
40
20
0
non targeting
sh-1
sh-2
Angpt2
C
Dnm1l
Fis1
Gene exp. (norm. to Actb)
0.015
0.010
0.005
0
0.07
*
0.10
0.08
0.06
0.04
0.02
D
Dnm1l
Fis1
0.15
0.10
0.05
**
E
Phospho ERK1/total ERK1
Phospho P38/total P38
2.5
2.0
1.5
1.0
0.5

Supplementary figure S7. Tumor cell-expressed *Angpt2* alters mitochondrial dynamics. (A) Representative electron microscopic images of control and *Angpt2*-deficient RET tumor cells kept under normoxic conditions. Square boxes depict ROIs at higher magnification. Scale bar: 2µm. **(B)** Quantitation of fragmented mitochondria per cell (n=19-20 cells/condition; mean ± SD). **(C)** *Dnm1l* and *Fis1* expression in control and *Angpt2* knockdown RET primary tumors was quantified using qRT-PCR (n=7-9; mean ± SD). *, p<0.05, Mann Whitney U test. **(D)** *Dnm1l* and *Fis1* expression in control and *Angpt2* knockdown B16F10 primary tumors was quantified using qRT-PCR (n=7-9; mean ± SD). *, p<0.05, **, p<0.01, Mann Whitney U test. **(E)** Densitometry quantitation of protein intensities on Western Blot (Figure 4H) was performed with Fiji. Dot plots show ratio of phospho to total ERK1 and P38 proteins. (n=6; mean ± SD). *, p<0.05, **, p<0.01, Mann Whitney U test.

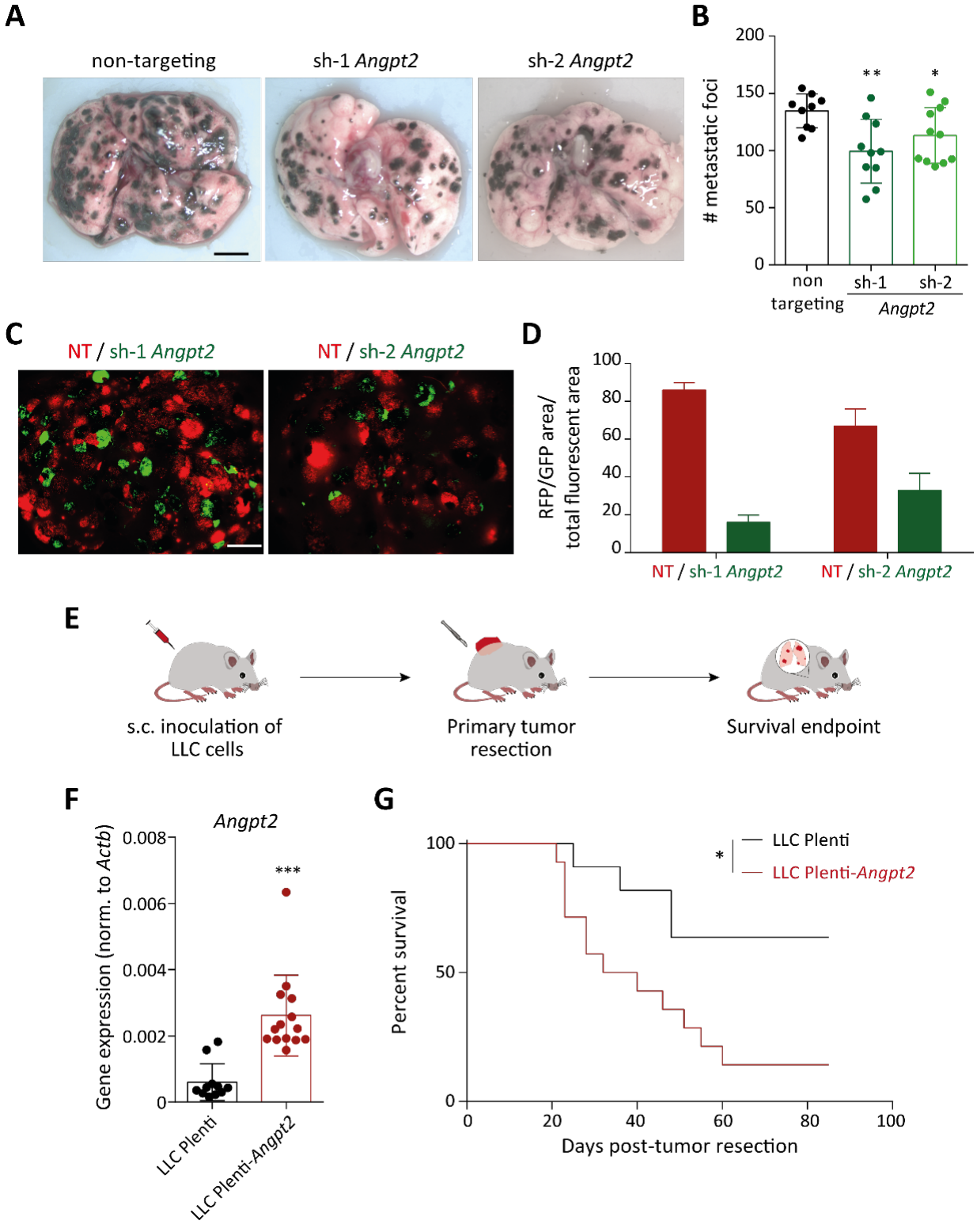
A
non-targeting
sh-1 Angpt2
sh-2 Angpt2
B
metastatic foci
200
150
100
50
0
**
*
non targeting
sh-1
sh-2
Angpt2
C
NT / sh-1 Angpt2
NT / sh-2 Angpt2
D
RFP/GFP area/ total fluorescent area
100
80
60
40
20
0
NT / sh-1 Angpt2
NT / sh-2 Angpt2
E
s.c. inoculation of LLC cells
Primary tumor resection
Survival endpoint
F
Angpt2
Gene expression (norm. to Actb)
0.008
0.006
0.004
0.002
0
***
LLC Plenti
LLC Plenti-Angpt2
G
Percent survival
100
50
0
0
20
40
60
80
100
Days post-tumor resection
*
LLC Plenti
LLC Plenti-Angpt2

Supplementary figure S8. Tumor cell-expressed *Angpt2* promotes metastasis. (A) Control or *Angpt2*-silenced B16F10 cells were injected into the tail vein of C57BL/6N mice. The mice were sacrificed after 14 days. Shown are representative images of lung metastatic foci imaged under a stereomicroscope. Scale bar: 5mm**. (B)** The graph represents the quantitation of lung metastatic foci (n=9-11; mean ± SD). *, p<0.05, **, p<0.01, Mann Whitney U test. **(C)** Control (in red) and *Angpt2*-silenced (in green) B16F10 tumor cells were co-injected intravenously in mice. Lungs were harvested 14 days after tumor cell inoculation and visualized under a fluorescent dissection microscope. Representative images of lung metastatic foci are shown. Scale bar: 2mm**. (D)** Quantitation of lung colonization by control (in red) or *Angpt2*-depleted (in green) B16F10 tumor cells. The area of each metastatic colony (RFP/GFP) was normalized to the combined fluorescent area (n=6; mean ± SD). **(E)** Schematic representation of the LLC spontaneous metastasis experiment. **(F)** *Angpt2* expression in control and *Angpt2*-overexpressing LLC primary tumors was quantified using qRT-PCR (n=11-14; mean ± SD). ***, p<0.001, Mann Whitney U test. **(G)** Kaplan-Meier plot showing percent survival of mice implanted with either control or *Angpt2*-overexpressing LLC tumor cells after primary tumor resection. *, P<0.01, Log-rank (Mantel-Cox) test.

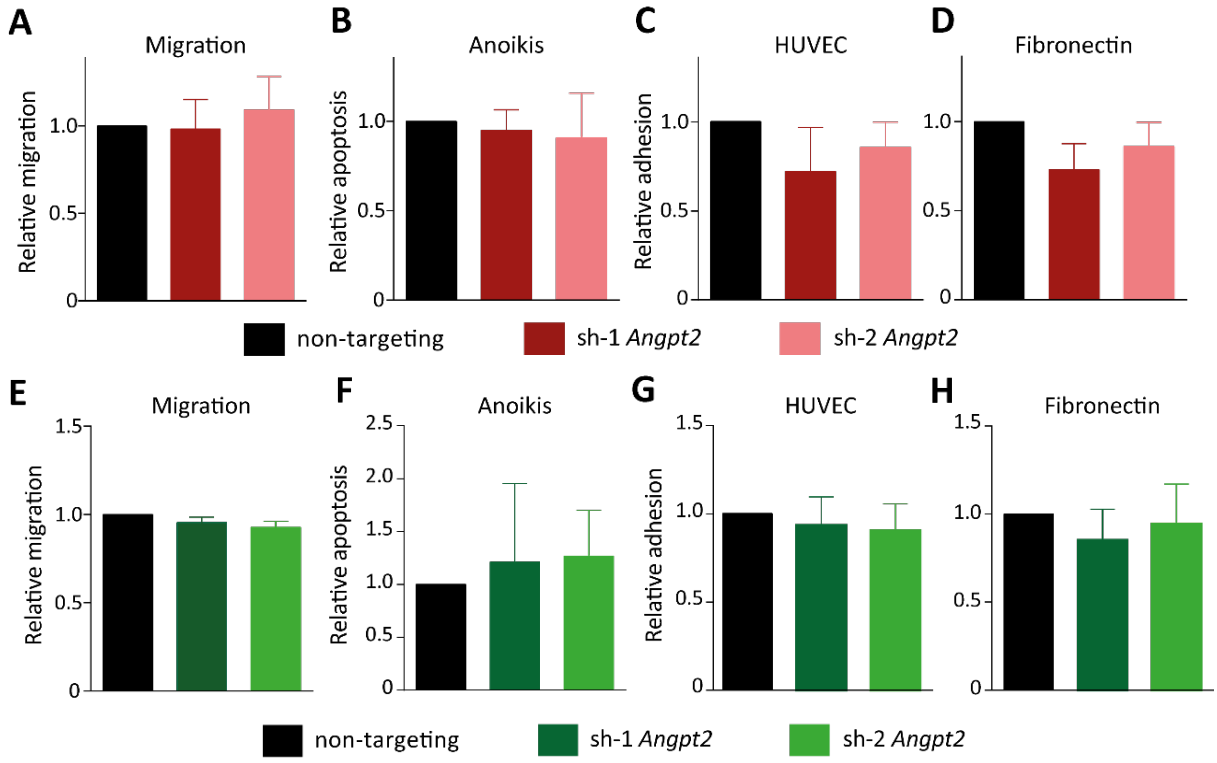

Supplementary figure S9. Tumor cell-expressed *Angpt2* does not affect early stages of metastasis *in vitro* (A,E, migration; B,F, anoikis; C,G, adhesion to EC; D,H, adhesion to fibronectin) of RET tumor cells (A-D) and B16F10 cells (E-H). **(A)** Control and *Angpt2*-deficient RET tumor cells were plated on Transwell (8 µm pore size) of cell invasion and migration (CIM) plates and their migration toward serum containing medium was monitored for 48h by impedance-based RTCA measurements (n=3; mean ± SD). **(B)** Control or *Angpt2*-silenced RET cells were grown on ultra-low attachment plates for 48h. Thereafter, cells were stained with Annexin V-APC and FxCycle to compute apoptotic cells by FACS (n=4; mean ± SD). **(C)** Control and *Angpt2* knockdown RET tumor cells were allowed to adhere for 40min on a mono-layer of HUVECs. Post-adhesion, non-adherent cells were removed and the fraction of adherent tumor cells was analyzed by FACS (n=4; mean ± SD). **(D)** Control or *Angpt2*-silenced RET cells were plated on Fibronectin-coated plates for 40min. Non-adherent cells were washed away and adherent cells were quantified by spectrophotometric analysis of crystal violet stain (n=3; mean ± SD). **(E)** Control or *Angpt2*-deficient B16F10 tumor cells were plated on Transwell (8 µm pore size) of CIM plates and their migration toward serum containing medium was monitored for 48h by impedance-based RTCA measurements (n=3; mean ± SD). **(F)** B16F10 cells were grown on ultra-low attachment plates for 48h. Thereafter, cells were stained with Annexin V-APC and FxCycle to compute apoptotic cells by FACS (n=4; mean ± SD). **(G)** Control and *Angpt2* knockdown B16F10 cells were allowed to adhere for 40min on a monolayer of HUVECs. Post-adhesion, non-adherent cells were removed, and the fraction of adherent tumor cells was quantitated by FACS (n=3; mean ± SD). **(H)** Control or *Angpt2*-silenced B16F10 cells were seeded on Fibronectin-coated plates for 40min. Non-adherent cells were washed away and adherent cells were quantified by spectrophotometric analysis of crystal violet stain (n=5; mean ± SD). **(A-H)** The data were normalized to the non-targeting shRNA controls.

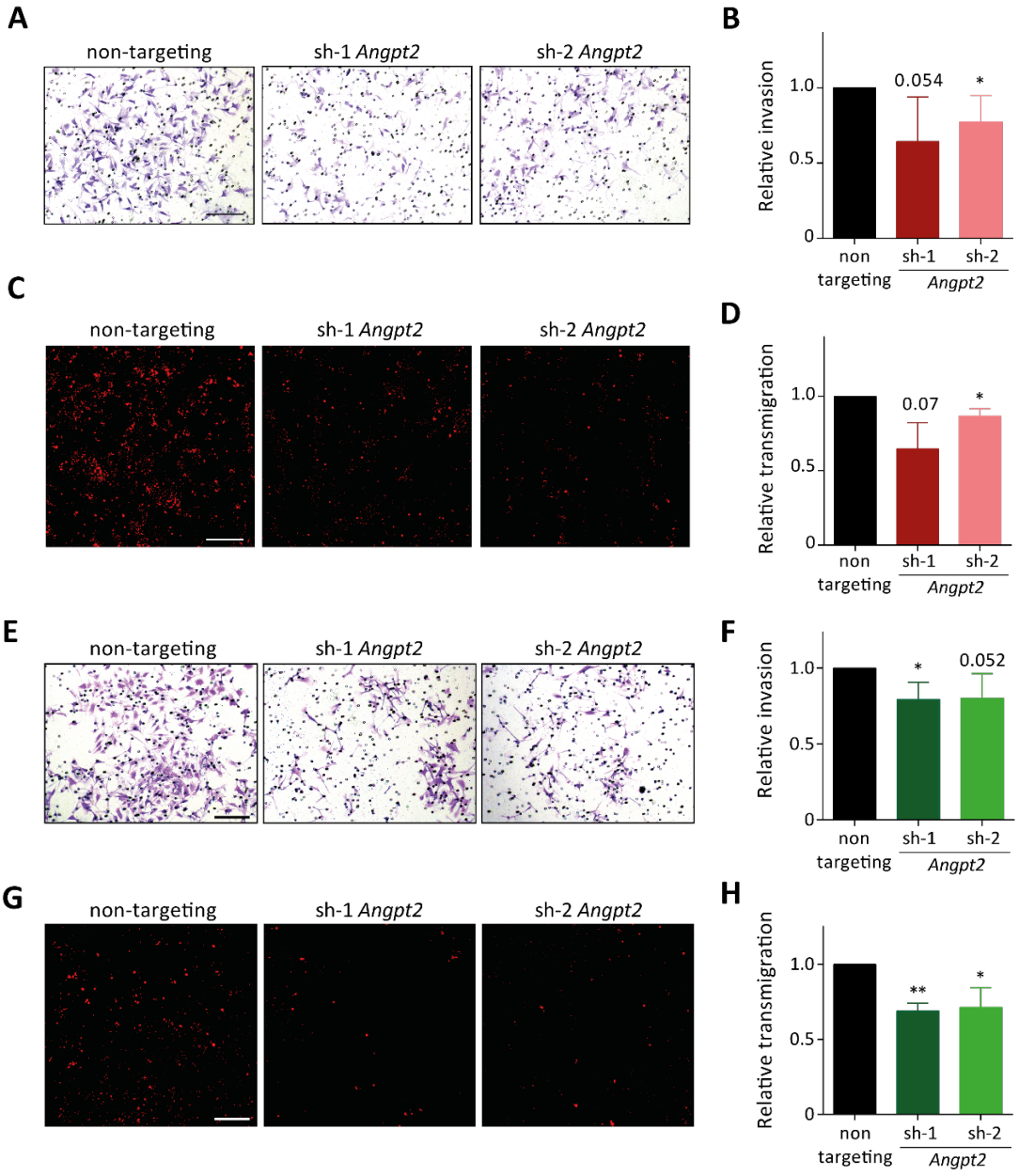
A
non-targeting
sh-1 Angpt2
sh-2 Angpt2
B
Relative invasion
1.0
0.5
0
0.054
*
non targeting
sh-1
sh-2
Angpt2
C
non-targeting
sh-1 Angpt2
sh-2 Angpt2
D
Relative transmigration
1.0
0.5
0
0.07
*
non targeting
sh-1
sh-2
Angpt2
E
non-targeting
sh-1 Angpt2
sh-2 Angpt2
F
Relative invasion
1.0
0.5
0
*
0.052
non targeting
sh-1
sh-2
Angpt2
G
non-targeting
sh-1 Angpt2
sh-2 Angpt2
H
Relative transmigration
1.0
0.5
0
**
*
non targeting
sh-1
sh-2
Angpt2

Supplementary figure S10. Silencing of *Angpt2* impairs invasion through the basement membrane and transmigration across the endothelial barrier of RET tumor cells (A-D) and B16F10 cells (E-H). **(A)** Representative images of control or *Angpt2*-depleted RET invaded cells. Scale bar: 100 µm. **(B)** Quantitation of invasiveness in control and *Angpt*-2 depleted RET cells (n=5; mean ± SD). *p<0.05, two-tailed paired Student's t-test. **(C)** Representative images show PKH-26 Red-labeled parental (non-targeting) and *Angpt2*-depleted transmigrated RET tumor cells on the lower side of the Transwell. Scale bar: 100 µm. **(D)** Quantification of transmigrated parental and knockdown (sh-1 and sh-2 *Angpt2*) tumor cells (n=3; mean ± SD). *p<0.05, two-tailed paired Student's t-test. **(E)** Representative images of control or *Angpt2*-depleted B16F10 invaded cells. Scale bar: 100 µm. **(F)** Quantitation of invasiveness in control and *Angpt*-2 depleted B16F10 cells (n=5; mean ± SD). *p<0.05, two-tailed paired Student's t-test. **(G)** Representative images show PKH-26 Red labeled parental (non-targeting) and *Angpt2*-depleted transmigrated B16F10 tumor cells on the lower side of the Transwell. Scale bar: 100 µm. **(H)** Quantification of transmigrated parental and knockdown (sh-1 and sh-2 *Angpt2*) tumor cells (n=4; mean ± SD). *p<0.05, **, p<0.01, two-tailed paired Student's t-test.

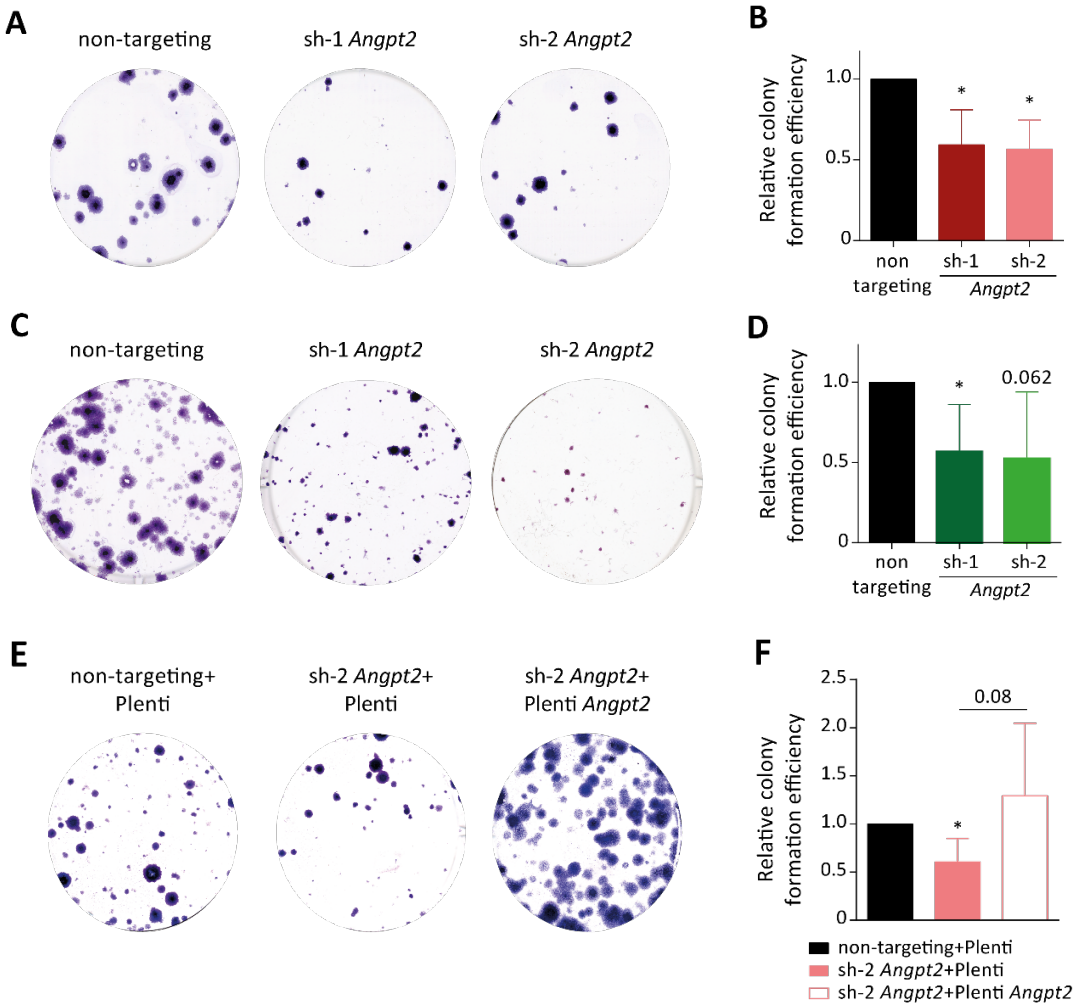

Supplementary figure S11. Silencing of *Angpt2* reduces *in* vitro colony formation of RET tumor cells (A,B,E,F) and B16F10 cells (C,D). **(A)** Control and *Angpt2*-silenced RET cells were cultured under anoikis conditions for 48h. Next, cells were harvested, and 600 cells were seeded in a 6-well plate for the colony formation assay. Shown are representative images from the colony formation assay. **(B)** The graph quantifies the number of colonies stained with crystal violet (n=4; mean ± SD). *p<0.05, two-tailed paired Student's t-test. **(C)** Control and *Angpt2*-silenced B16F10 cells were cultured under anoikis condition for 48h. Next, cells were harvested and 600 cells were seeded in a 6-well plate for the colony formation assay. Shown are representative images from the colony formation assay. **(D)** The graph quantifies the number of colonies as stained with crystal violet (n=5; mean ± SD). *p<0.05, two-tailed paired Student's t-test. **(E)** Representative images from the colony formation assay of control+Plenti, sh-2+Plenti and sh-2+Plenti *Angpt2* RET tumor cells. **(F)** The graph quantifies the number of colonies stained with crystal violet (n=5; mean ± SD). *p<0.05, two-tailed paired Student's t-test. **(A-F)** The data were normalized to the non-targeting shRNA controls.